RM L52H06a

NACA

RESEARCH MEMORANDUM

FREE-FLIGHT MEASUREMENTS OF SOME EFFECTS OF SPOILER SPAN AND PROJECTION AND WING FLEXIBILITY ON ROLLING EFFECTIVENESS AND DRAG OF PLAIN SPOILERS ON A TAPERED SWEPTBACK WING AT MACH NUMBERS BETWEEN 0.6 AND 1.6

By Eugene D. Schult and E. M. Fields

Langley Aeronautical Laboratory
Langley Field, Va.

NATIONAL ADVISORY COMMITTEE
FOR AERONAUTICS

WASHINGTON

October 3, 1952
Declassified August 16, 1957

NATIONAL ADVISORY COMMITTEE FOR AERONAUTICS

RESEARCH MEMORANDUM

FREE-FLIGHT MEASUREMENTS OF SOME EFFECTS OF SPOILER SPAN AND PROJECTION AND WING FLEXIBILITY ON ROLLING EFFECTIVENESS AND DRAG OF PLAIN SPOILERS ON A TAPERED SWEPTBACK WING AT MACH NUMBERS BETWEEN 0.6 AND 1.6

By Eugene D. Schult and E. M. Fields

SUMMARY

As a part of the transonic research program of the National Advisory Committee for Aeronautics, the Pilotless Aircraft Research Division has conducted a free-flight investigation to determine some effects of spoiler span, spanwise location, projection, and wing flexibility on the drag and rolling effectiveness of spoilers through the Mach number range between 0.6 and 1.6. The wings were swept back 45° along the quarter-chord line, had an aspect ratio of 4.0, taper ratio of 0.6, and NACA 65A006 airfoil sections parallel to the free stream. The solid, sharp-edged spoilers were located along the 70-percent-chord line. Test results indicated that the full-span spoiler had the highest rolling effectiveness for a given projection of all configurations at all speeds tested and that the inboard half-span spoilers were approximately twice as effective as the outboard half-span spoilers. The outboard quarter-span spoilers were not effective as roll-producing devices. The variation of rolling effectiveness with spoiler projection was nonlinear at subsonic speeds but became approximately linear at supersonic speeds. An increase in spoiler span gave more rolling effectiveness per unit drag than did an increase in spoiler projection. A comparison of spoilers and ailerons at the same rolling effectiveness indicated that the spoiler had lower wing twisting moments and greater drag than the aileron; however, for the inboard control the difference in drag between spoilers and ailerons became small at supersonic speeds.

INTRODUCTION

The greater wing flexibilities normally associated with the thinner airfoil sections point out a basic need for lateral-control devices which maintain a high level of rolling effectiveness without producing adverse wing twisting moments. Comparative tests of spoiler and flap-type controls at transonic and supersonic speeds (ref. 1) show that spoilers have considerably smaller aeroelastic losses in rolling effectiveness than flap-type controls. In order to obtain more information on spoiler controls, the Langley Pilotless Aircraft Research Division has conducted experimental investigations to determine the rolling effectiveness and drag of various plain-spoiler configurations at Mach numbers between 0.6 to 1.6. Continuous data over the Mach number range were obtained with rocket-propelled test vehicles in free flight by means of the technique described in reference 2.

Some effects of spoiler projection, span, and location on rolling effectiveness and drag were determined for spoilers located along the 70-percent wing-chord line. The wings were swept back 45° along the quarter-chord line, had an aspect ratio of 4.0, taper ratio of 0.6, and NACA 65A006 airfoil sections parallel to the free stream. The effects of wing torsional flexibility on the rolling effectiveness and drag of the outboard partial-span spoiler, and some drag comparisons between spoiler- and aileron-type controls having the same rolling effectiveness are also included.

SYMBOLS

A	aspect ratio, $\frac{b^2}{S} = 4.0$
b	diameter of circle swept by wing tips, 3.0 ft
S	area of two wings measured to model center line, 2.25 sq ft
S'	exposed area of three wings, 2.80 sq ft
c	local wing chord measured parallel to model center line, ft
M	Mach number
q	dynamic pressure, lb/sq ft
V	flight-path velocity, ft/sec

R	Reynolds number of tests based on average exposed wing chord (0.72 ft)
p	rolling velocity, positive for right wing moving downward as seen from rear, radians/sec
$pb/2V$	wing-tip helix angle, radians
h	local spoiler height above wing, measured normal to wing-chord plane (spoiler is on upper surface when wing is on right), ft
i_w	average wing incidence per wing from three wings, measured in plane normal to wing-chord plane and parallel to free stream, positive if tending to produce positive p, deg
y	spanwise distance, measured from and normal to model center line, ft
s	control span, measured in direction of y, ft
m	concentrated couple, applied near wing tip in plane parallel to free stream and normal to the wing-chord plane, ft-lb
θ	angle of twist produced by m at any section along wing span and measured parallel to plane of m, radians
(θ/m)	wing torsional flexibility parameter, radians/ft-lb
λ	wing taper ratio (ratio of tip chord to chord at model center line), 0.6
δ	deflection of aileron, measured normal to hinge line, deg
C_D	drag coefficient, $\frac{\text{Drag}}{qS'}$
ΔC_D	incremental drag coefficient of three spoilers (one per wing)

Subscripts:

i	inboard when used in conjunction with control span
R	rigid-wing data
F	flexible-wing data

MODELS AND TECHNIQUE

A typical three-winged test vehicle of the type used in the present investigation is illustrated in the photograph presented as figure 1. The wings were swept back 45° along the quarter-chord line, had an aspect ratio of 4.0, taper ratio of 0.6, and NACA 65A006 airfoil sections parallel to the free stream. The geometric characteristics of the test configurations are given in table I and in figure 2. The spoilers were located along the 70-percent-chord line of each wing and had projections of 2-percent and 5-percent chord. In order to determine some effects of wing flexibility on the rolling effectiveness and drag, three different wing stiffnesses were tested in conjunction with the outboard $0.43\frac{b}{2}$ - span spoiler (fig. 2). Measured values of the variation with span of the wing torsional flexibility parameter θ/m are plotted in figure 3.

The flight tests were made at the Pilotless Aircraft Research Station at Wallops Island, Va. A two-stage rocket-propulsion system propelled the models to a maximum Mach number of approximately 1.6. During approximately 12 seconds of coasting flight following propellant burnout, time-history measurements were made of the flight-path velocity with a CW Doppler radar set and of rolling velocity with special radio equipment. These data, in conjunction with atmospheric data obtained with radiosondes, permit the evaluation of the drag coefficient C_D and rolling effectiveness parameter $(pb/2V)_F$ as a function of Mach number. Reference 2 gives a more complete description of the flight-testing technique.

The Reynolds number based on average wing chord varied from approximately 2×10^6 to 8×10^6 over the Mach number range, and the maximum variation of dynamic pressure for all configurations at a given Mach number was of the order of ±70 pounds per square foot from the mean (fig. 4).

ACCURACY AND CORRECTIONS

From previous experience and mathematical analysis, the experimental uncertainties in the test variables are believed to be within the following limits:

	Subsonic	Supersonic
M	± 0.010	± 0.005
C_D	$\pm .003$	$\pm .002$
$(pb/2V)_F$	$\pm .003$	$\pm .002$

The sensitivity of the experimental technique is such that small irregularities in the variation of $pb/2V$ with Mach number in the order of one-half the magnitude shown above, however, may be detected. The maximum uncertainties in the determination of i_W and h/c are $\pm 0.05^\circ$ and ± 0.001, respectively.

All $(pb/2V)_F$ values presented herein have been corrected for the effects of wing incidence due to construction tolerances (see table I) by the method outlined in reference 3.

RESULTS AND DISCUSSION

The results of this investigation are presented in figures 5 to 13. The basic-data plots of test vehicle total drag coefficient C_D and flexible wing rolling effectiveness $(pb/2V)_F$ are presented in figure 5 for various plain-spoiler controls with projections of 2 percent and 5 percent of the local wing chord. All models had wings of the same stiffness characteristics except models 7 and 8 which had reduced wing stiffnesses.

Rolling Effectiveness

Effect of wing flexibility.- Figure 5(b) shows some effects of wing flexibility on the rolling effectiveness for the outboard half-span spoiler. From these data the fraction of rigid-wing rolling effectiveness retained by a flexible wing of type "A" construction was calculated by the method of reference 1 and is shown in figure 6 along with data for an aileron-equipped wing of the same construction. Figure 6 shows that the percent of rigid-wing rolling effectiveness lost for the spoiler wing is less than one-half that of the aileron wing for the same wing stiffness and approximately the same $pb/2V$ at $M \geq 1.1$. Since this loss is due primarily to the wing twisting moment in the free-stream direction (ref. 1), the wing twisting moment for the spoiler is less than one-half that for the aileron. When compared with the rigid wing, the effectiveness of the spoiler-equipped flexible wing was about 10 percent higher at $M = 0.6$ and 10 percent lower at $M = 1.6$; this condition indicates a change in the sign of the wing twisting moments as speed is increased through the transonic region.

Effect of spoiler span.- Figure 5 shows that, for a given spoiler projection and wing stiffness, the highest rolling effectiveness is obtained for the full-span spoilers over the Mach number range tested and that the inboard half-span spoiler has approximately twice the rolling effectiveness of the outboard half-span spoiler. The trend toward low or reversed rolling effectiveness for the outboard spoiler elements can be seen in figure 7 where rolling effectiveness is plotted as a function of outboard-spoiler span at various Mach numbers. These results show that the rolling effectiveness decreases almost linearly with decreasing outboard-spoiler span except near the wing tip where the short-span spoilers gave reversed rolling effectiveness at subsonic speeds and very low positive effectiveness at supersonic speeds. A tendency toward roll reversal was previously observed at subsonic speeds for unswept wings in free-flight tests of full-span spoilers having $\frac{1}{2}$-percent-chord projection (ref. 4) and also in full-scale flight tests of outboard part-span spoilers at small projections (ref. 5). This tendency toward roll reversal for low spoiler projections at subsonic speeds may be due to an effective cambering of the wing caused by spoiler projections that do not extend beyond the boundary layer (ref. 5). Figure 7 shows that the rolling effectiveness reversal for the present tests varies with both spoiler span and spoiler projection and occurs over a decreasing outboard spoiler span as either the Mach number or the spoiler projection is increased.

The rolling effectiveness of an inboard spoiler was estimated from the data of figures 5 and 7, and a comparison with measured values is presented in figure 8. The method of combining the effectiveness of individual control segments into a single spanwise influence curve, although not generally applicable for spoilers at subsonic speeds, as indicated by figure 8 and references 6 and 7, gave good results at transonic speeds and fair results at supersonic speeds for the spoilers. Tests with an aileron control (ref. 8) show good agreement throughout the Mach number range when a comparison is made between the rolling effectiveness values as measured and as estimated from a single spanwise influence curve.

Effect of spoiler projection.- Figure 9 shows the effect of spoiler height on the rolling effectiveness at various Mach numbers for each configuration tested. At high subsonic and transonic speeds the rolling effectiveness of all configurations is shown to change with spoiler height in a nonlinear fashion. There is a general decrease in the rate of change of rolling effectiveness with spoiler height at the higher projections except for the outboard quarter-span spoiler. As the Mach number is increased between $M \approx 1.1$ and $M \approx 1.5$, the results indicate that the rolling effectiveness variation with spoiler projection becomes more nearly linear for all configurations tested.

Drag

Effect of wing flexibility.- Figure 5(b) shows negligible variations in test-vehicle total drag coefficient for the outboard half-span spoiler when the wing torsional stiffness is reduced by a factor of approximately 2.5.

Effect of spoiler span.- In figure 10 some effects of Mach number and outboard spoiler span on the incremental drag coefficient ΔC_D are presented for spoiler projections of 2-percent and 5-percent chord. The ΔC_D values were obtained by subtracting the total drag of a test vehicle without spoilers from the total drag of the test vehicles with spoilers. The total drag of the test vehicle without spoilers (fig. 5) may be considered to be essentially the same as zero-roll drag, since the induced-drag effects of the preset 1.4° incidence were decreased when the model was free to roll and are believed to be small. Thus, the incremental drag coefficient ΔC_D represents primarily the drag due to the addition of the spoilers (one per wing) plus an induced drag component due to the net lift distribution which exists over the rolling wing. The difference in drag coefficient associated with the slight difference in flexibility between the solid duralumin wings (ref. 8) and type "A" wings of the present tests is believed to be small. Results in figure 10 indicate a general decrease in incremental spoiler drag increment with increase in Mach number and show an almost linear increase of spoiler drag increment with increasing span of outboard spoilers over the Mach number range tested. In figure 11, the incremental spoiler drag coefficient ΔC_D is plotted against spoiler height for all spoiler configurations and results show that, for a given spoiler projection, the drag of the full-span spoiler is slightly less than the sum of the drag values of its inboard and outboard components measured individually at all Mach numbers tested.

Effect of spoiler projection.- At subsonic speeds, figure 11 shows that ΔC_D increases almost linearly with increased spoiler projection for all spoiler configurations tested. At transonic and supersonic speeds the variation of ΔC_D with spoiler height remains linear for the outboard spoiler segments but becomes nonlinear for the inboard and full-span spoilers. Slight additional drag increases are noted at $\frac{h}{c} \approx 0.05$ for the inboard spoilers and for the inboard elements of the full-span spoiler (fig. 10) at transonic and supersonic speeds.

Drag comparison for spoiler and aileron.- The comparative drag between spoiler and aileron configurations having the same rolling effectiveness is presented as a function of Mach number in figure 12. The rolling-effectiveness data for the 0.3-chord aileron deflected 5° are taken from reference 8, and the drag data for the aileron configurations are unpublished. The drag values for the spoiler configurations were obtained from the present test results by plotting $(pb/2V)_F$ against C_D at constant Mach number and interpolating for C_D at the desired $(pb/2V)_F$. Figure 12 shows that the spoiler has more drag than the aileron for the same rolling effectiveness, but this difference becomes small at supersonic speeds especially for the inboard half-span control.

Variation of Rolling Effectiveness With Spoiler Drag

Figure 13 presents the rolling effectiveness data of each spoiler configuration plotted against the incremental spoiler-drag coefficient ΔC_D.

The solid curves of figure 13 represent constant-span spoilers with varying projections and the broken curves represent constant-projection spoilers with varying outboard spans. The curves were faired between test points by utilizing values from the faired curves of figures 7, 9, 10, and 11. The results show that, for the same ΔC_D, the full-span spoiler maintained the highest rolling effectiveness of all configurations tested up to a Mach number of approximately 1.5 where the inboard half-span spoiler became the most effective per unit drag. For a given drag increment the solid curves indicate that the inboard half-span spoiler produced almost twice the rolling effectiveness of an outboard half-span spoiler at all Mach numbers. In the transonic region, the variation of rolling effectiveness with drag in figure 13 indicates that, for $\frac{h}{c} \geq 0.05$, increases in spoiler height will probably result in relatively large drag increases but small rolling effectiveness increases. The data of figure 13 also indicate that a spoiler of low projection and large span would have less drag for the same rolling effectiveness than a short-span spoiler of large projection.

CONCLUSIONS

A free-flight investigation employing the rocket-model technique was made over the Mach number range from 0.6 to 1.6 to determine some effects of spoiler span, spanwise location and projection, and wing flexibility on the rolling effectiveness and drag of plain spoilers located along the 70-percent-chord line. Spoilers with projections of 2-percent and 5-percent chord were tested. The wings were swept back 45° along the quarter chord, had an aspect ratio of 4.0, taper ratio of 0.6, and NACA 65A006 airfoil sections. From the results of these tests the following conclusions have been drawn:

1. The full-span spoiler had the highest rolling effectiveness for a given projection of all configurations at all speeds tested.

2. For the same projection in percent chord, the inboard half-span spoiler had about twice the rolling effectiveness of the outboard half-span spoiler. Quarter-span spoilers at the wing tip had low effectiveness at supersonic speeds and reversed effectiveness at subsonic speeds.

3. The variation of rolling effectiveness with spoiler projection was generally linear at supersonic speeds but nonlinear at subsonic and transonic speeds.

4. For a given drag increment, the full-span spoiler had the largest rolling effectiveness at all speeds below $M \approx 1.5$; at this speed the inboard half-span spoiler had the largest rolling effectiveness per unit drag. Increases in spoiler span gave more rolling effectiveness per unit drag than did increases in spoiler projection.

5. A comparison of spoilers and ailerons at the same rolling effectiveness indicated that the spoiler had lower wing twisting moments but greater drag than the aileron; however, the drag difference between spoilers and ailerons became small at supersonic speeds for the inboard half-span control.

Langley Aeronautical Laboratory,
National Advisory Committee for Aeronautics,
Langley Field, Va.

REFERENCES

1. Strass, H. Kurt: Summary of Some Effective Aerodynamic Twisting-Moment Coefficients of Various Wing-Control Configurations at Mach Numbers From 0.6 to 1.7 as Determined From Rocket-Powered Models. NACA RM L51K20, 1952.

2. Sandahl, Carl A., and Marino, Alfred A.: Free-Flight Investigation of Control Effectiveness of Full-Span 0.2-Chord Plain Ailerons at High Subsonic, Transonic, and Supersonic Speeds To Determine Some Effects of Section Thickness and Wing Sweepback. NACA RM L7D02, 1947.

3. Strass, H. Kurt, and Marley, Edward T.: Rolling Effectiveness of All-Movable Wings at Small Angles of Incidence at Mach Numbers From 0.6 to 1.6. NACA RM L51H03, 1951.

4. Fields, E. M.: Some Effects of Spoiler Height, Wing Flexibility, and Wing Thickness on Rolling Effectiveness and Drag of Unswept Wings at Mach Numbers Between 0.4 and 1.7. NACA RM L52H18, 1952.

5. Kramer, Max, Zobel, Theodor W., and Esche, C. G.: Lateral Control by Spoilers at the DVL. NACA TM 1307, 1951.

6. Bollech, Thomas V., and Pratt, George L.: Effects of Plain and Step Spoiler Location and Projection on the Lateral Control Characteristics of a Plain and Flapped 42° Sweptback Wing at Reynolds Number of 6.8×10^{6}. NACA RM L9L20a, 1950.

7. Fischel, Jack, and Hammond, Alexander D.: Investigation of Effect of Span and Spanwise Location of Plain and Stepped Spoiler Ailerons on Lateral Control Characteristics of a Wing With Leading Edge Swept Back 51.3°. NACA RM L9K02, 1950.

8. Schult, Eugene D., Strass, H. Kurt, and Fields, E. M.: Free-Flight Measurements of Some Effects of Aileron Span, Chord, and Deflection and of Wing Flexibility on the Rolling Effectiveness of Ailerons on Sweptback Wings at Mach Numbers Between 0.8 and 1.6. NACA RM L51K16, 1952.

TABLE I

CONFIGURATIONS TESTED

Configuration	Model	$y_i/\frac{b}{2}$	$y_o/\frac{b}{2}$	h/c	i_w deg	Wing (a)
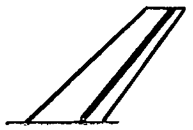	1	0.140	1.00	0.02	-0.04	A
	2	.140	1.00	.05	.10	A
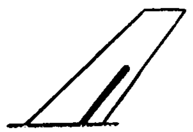	3	.140	0.57	.02	-.06	A
	4	.140	0.57	.05	-.06	A
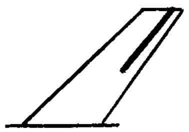	5	.570	1.00	.02	-.04	A
	6	.570	1.00	.05	-.02	A
	7	.570	1.00	.05	.02	B
	8	.570	1.00	.05	-.05	C
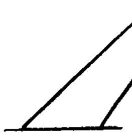	9	.785	1.00	.02	-.03	A
	10	.785	1.00	.05	-.11	A

NACA

(a) See Fig. 2.

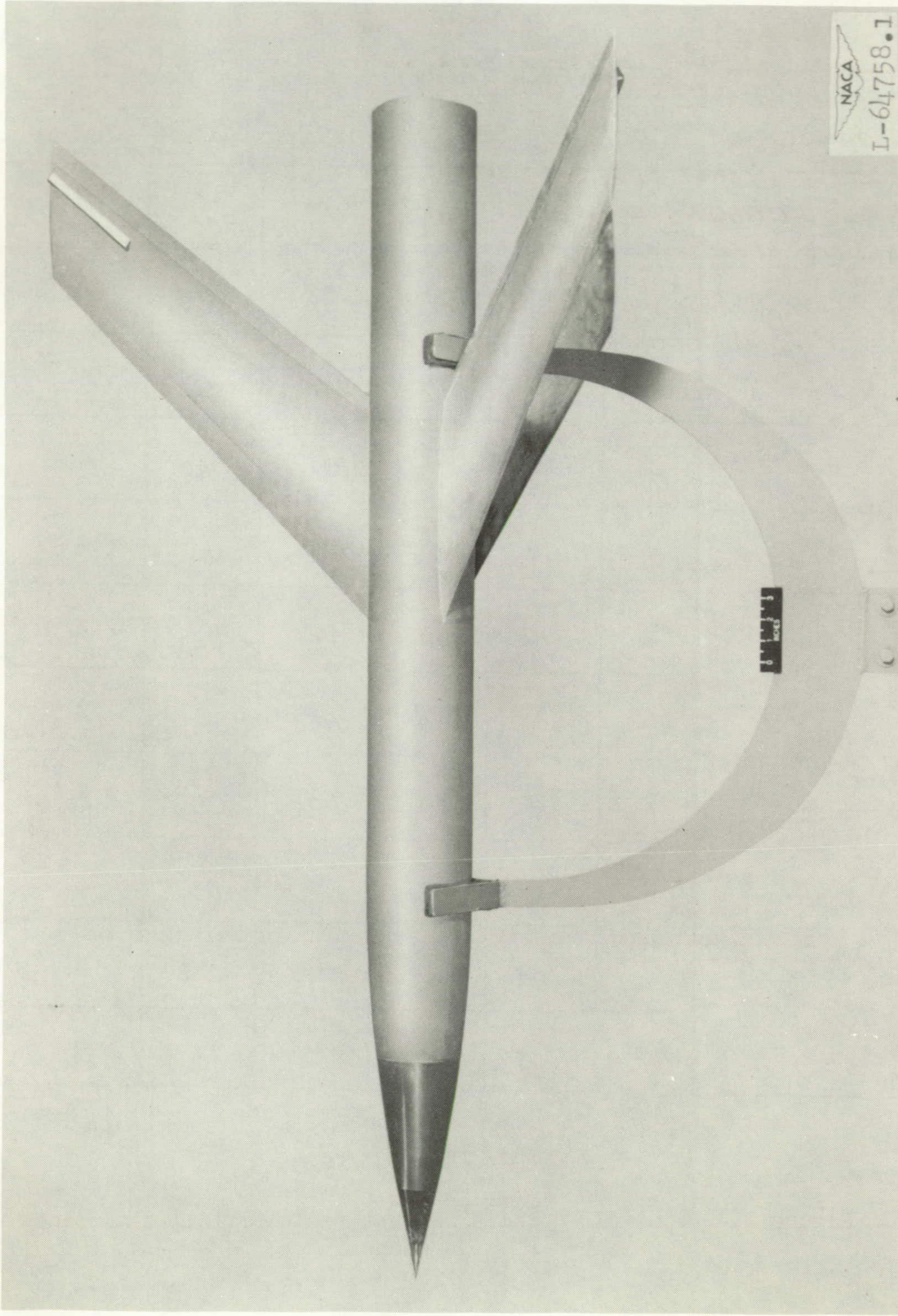

Figure 1.- Typical test vehicle (three wings).

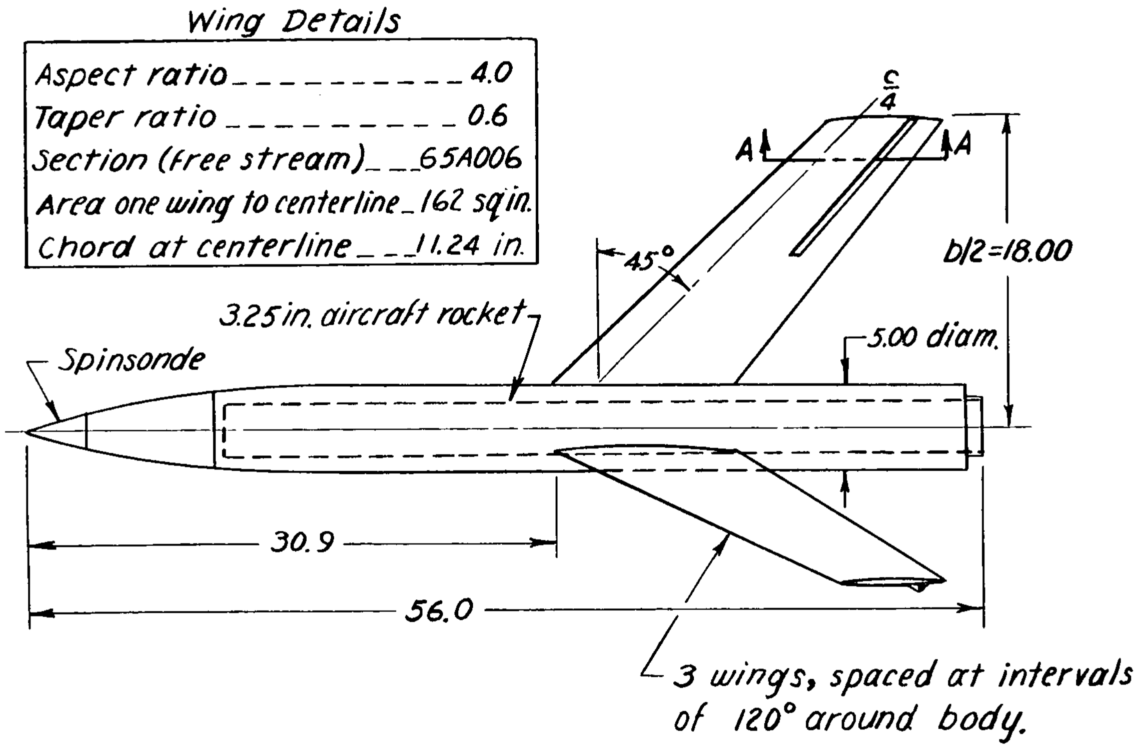

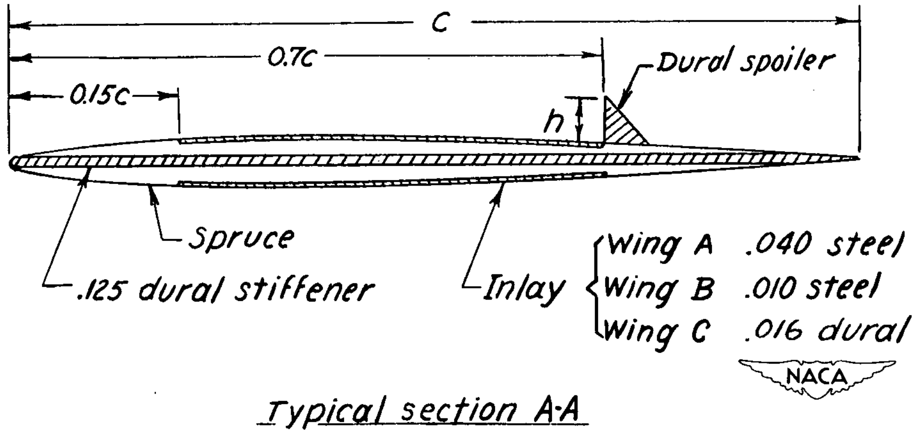

Figure 2.- Geometric details of test vehicle. All dimensions are in inches.

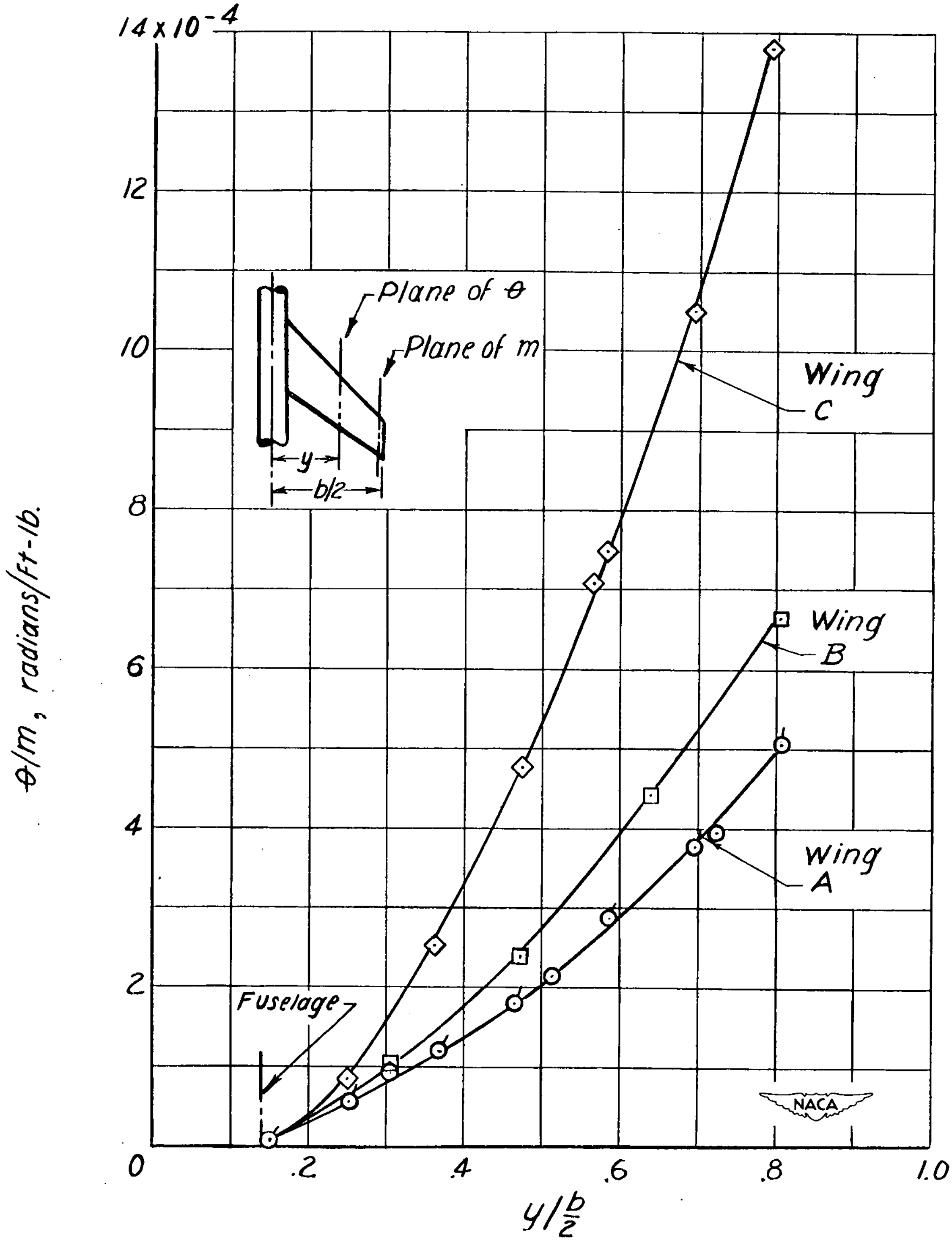

Figure 3.- Variation of wing torsional flexibility parameter with wing span. Couple applied near wing tip in a plane parallel to body axis and normal to wing-chord plane.

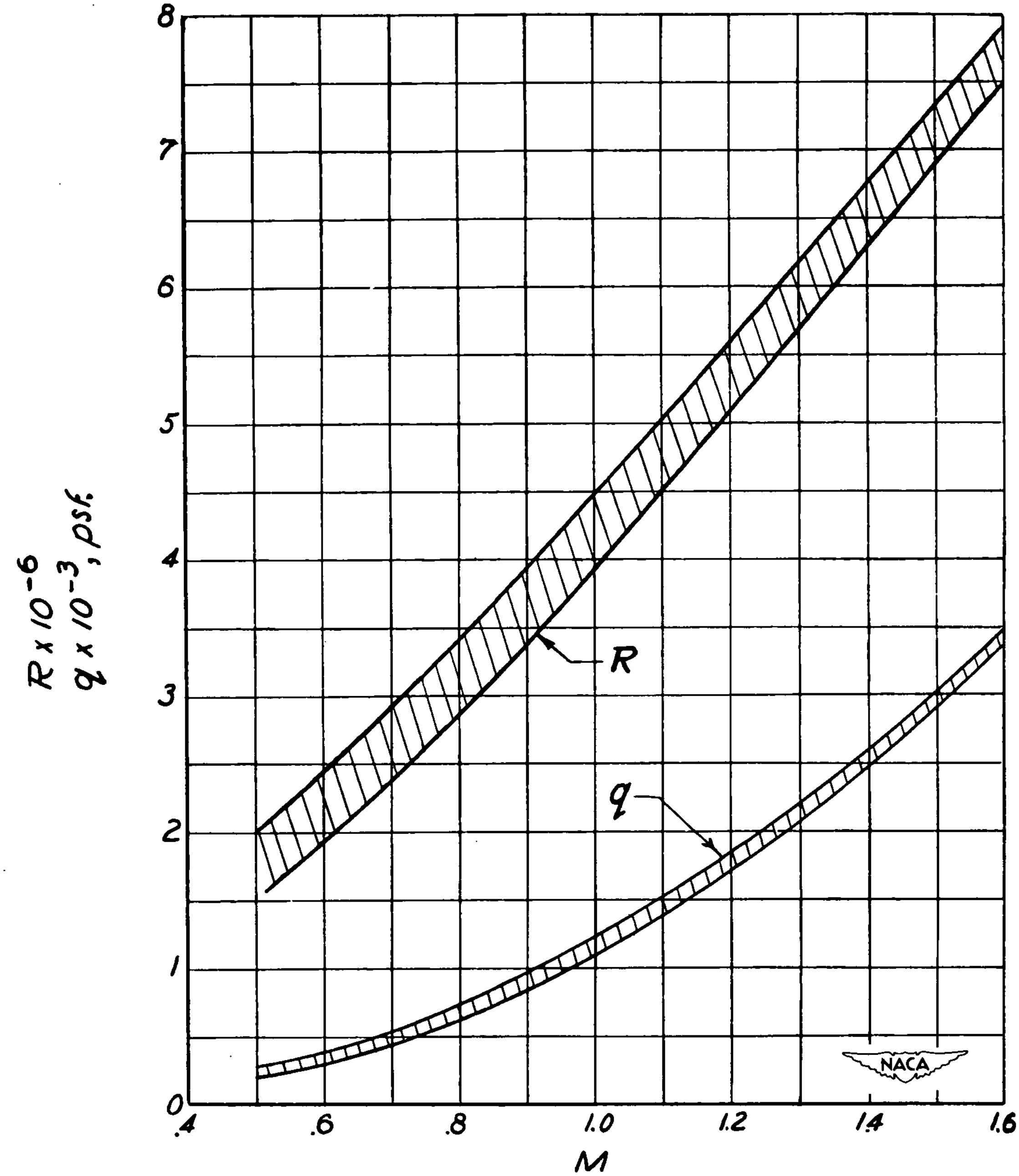

Figure 4.- Variation of test Reynolds number and dynamic pressure with Mach number. Reynolds number based upon average wing chord of 0.72 foot.

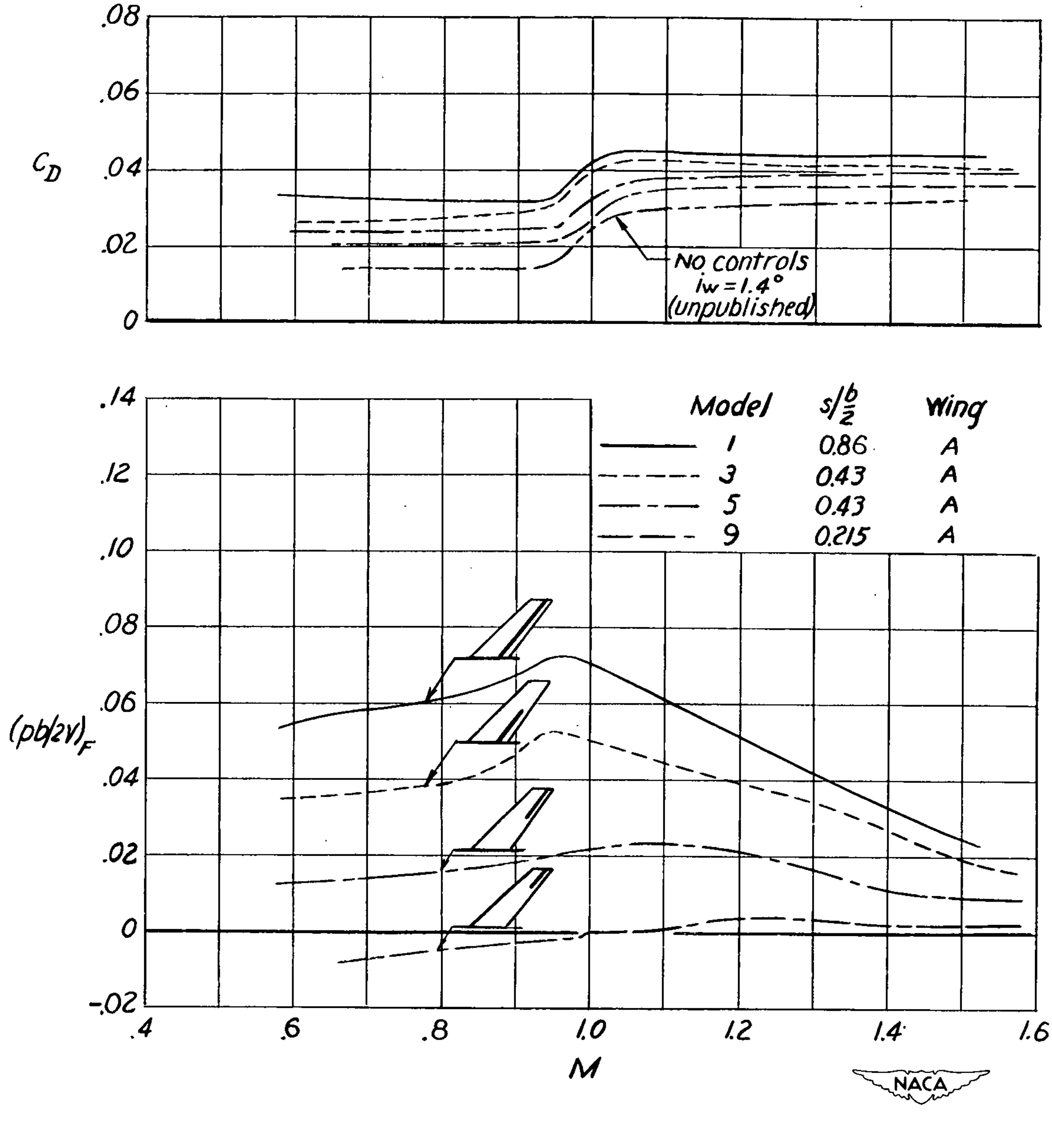

(a) $\frac{h}{c} = 0.02$.

Figure 5.- Variation of total drag coefficient and rolling effectiveness with Mach number for various spoilers located at the 70-percent-chord line. $i_W = 0$.

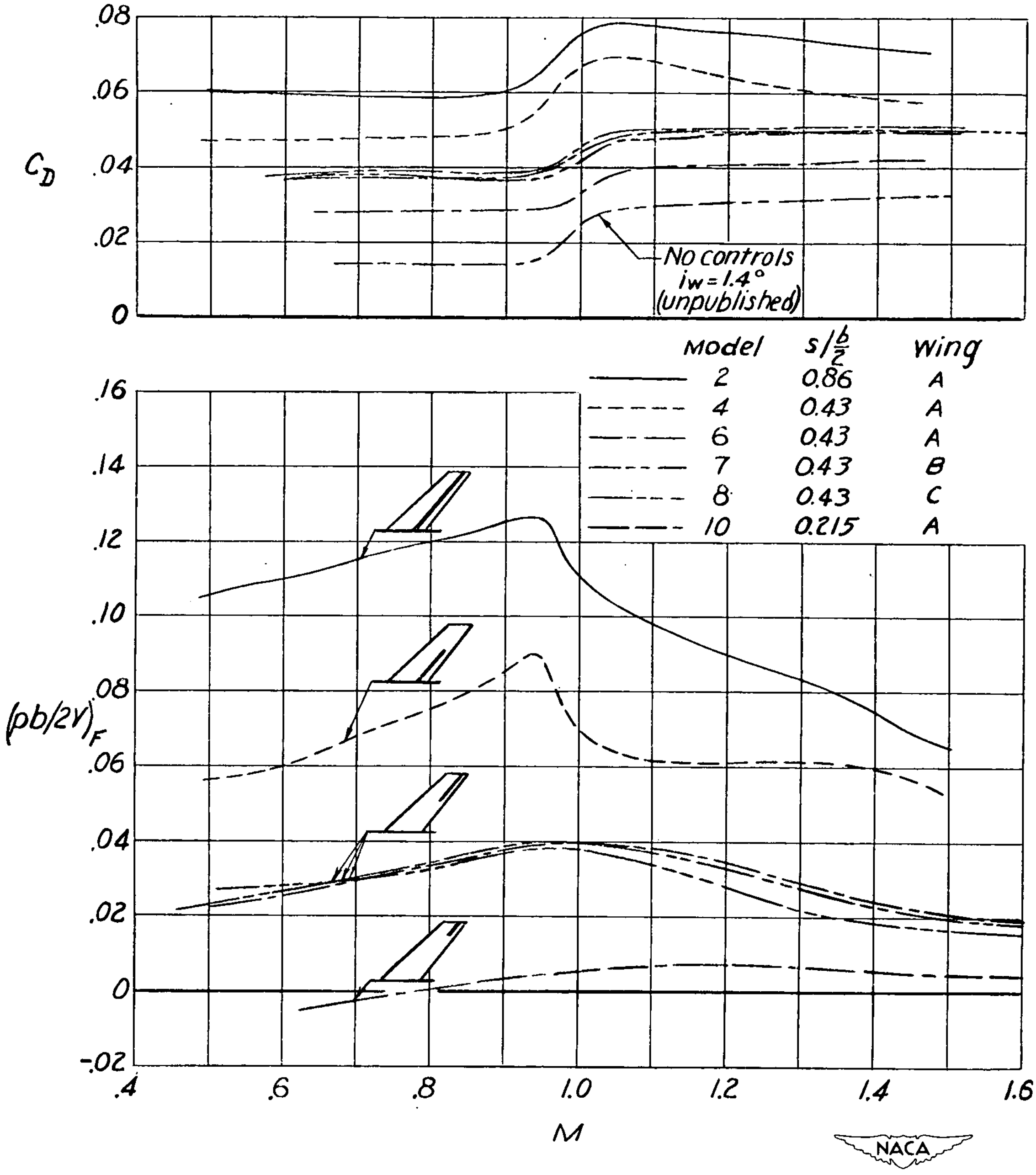

(b) $\frac{h}{c} = 0.05.$

Figure 5.- Concluded.

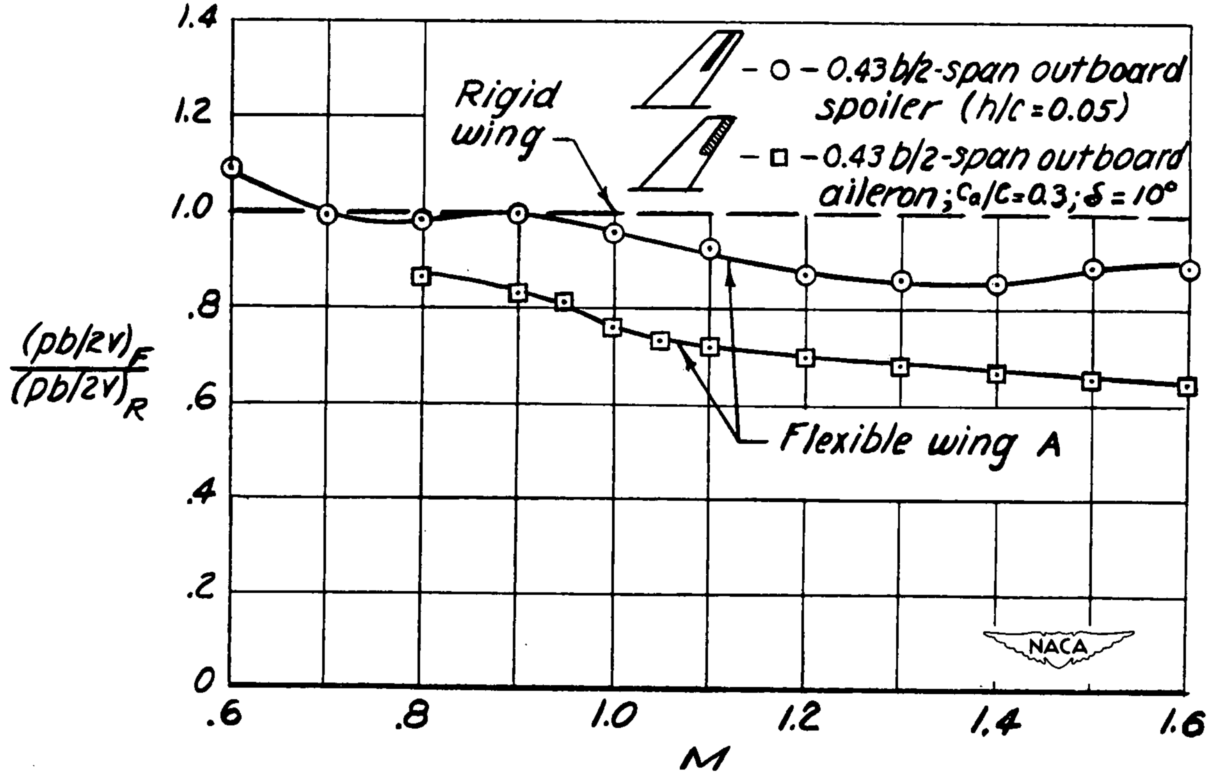

Figure 6.- Variation with Mach number of the fraction of rigid-wing rolling effectiveness retained by either spoilers or ailerons on flexible wing A. Aileron data from reference 8; both controls had approximately the same $pb/2V$ at $M \geq 1.1$.

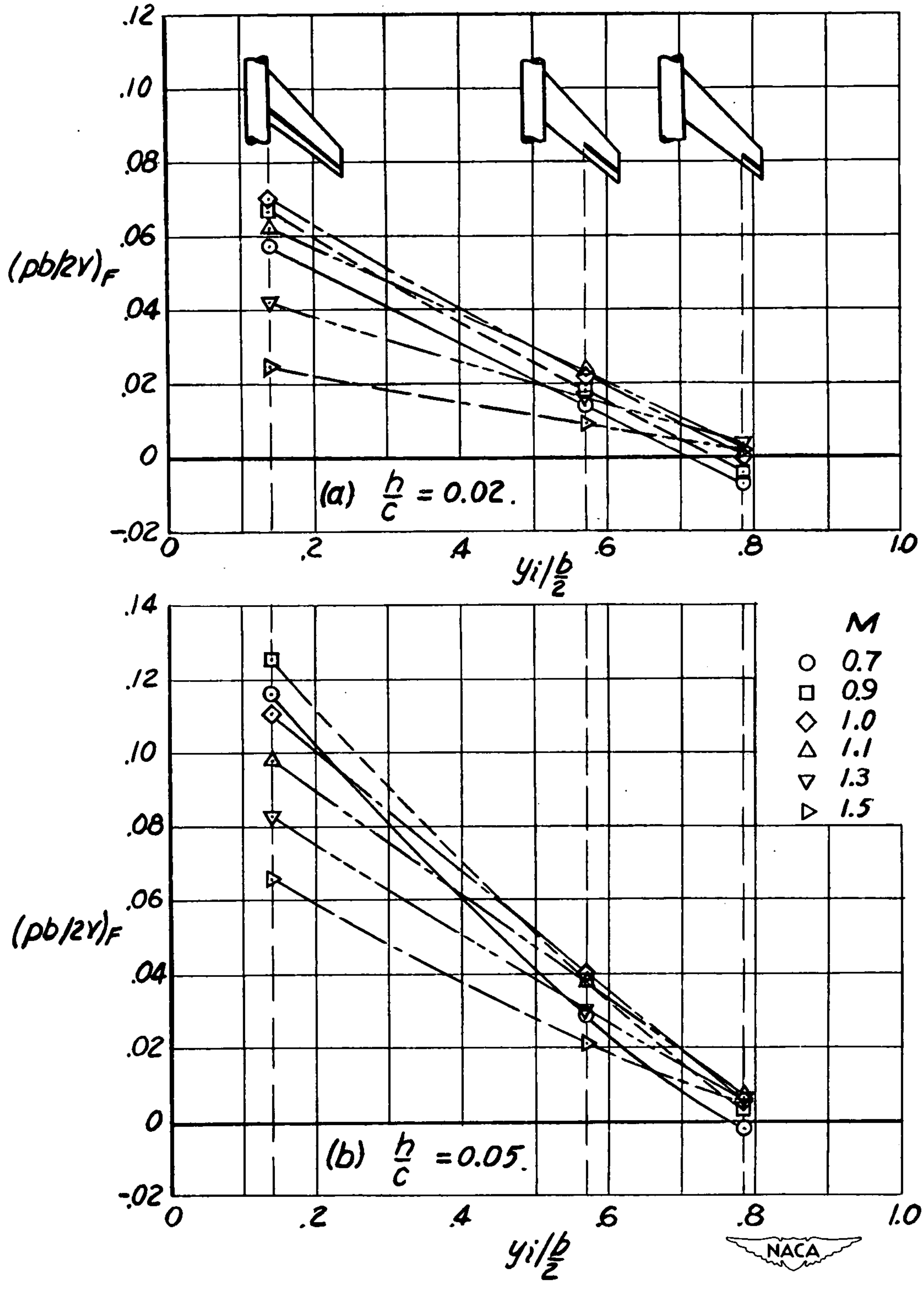

Figure 7.- Rolling effectiveness as a function of outboard spoiler span at constant Mach number and for both projections tested. Type A wing structure.

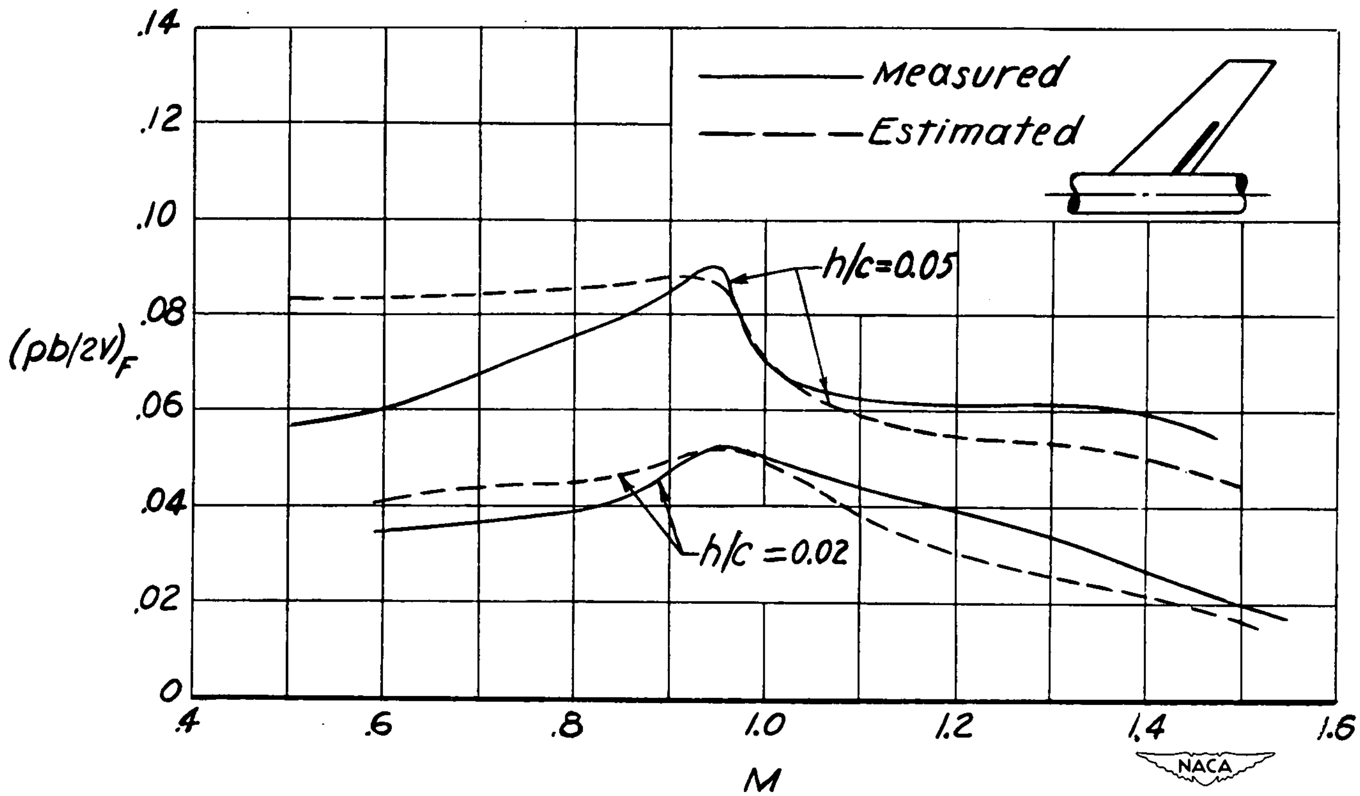

Figure 8.- Variation with Mach number of the measured rolling effectiveness of an inboard $0.43\frac{b}{2}$ - span spoiler compared with values estimated from figures 5 and 7.

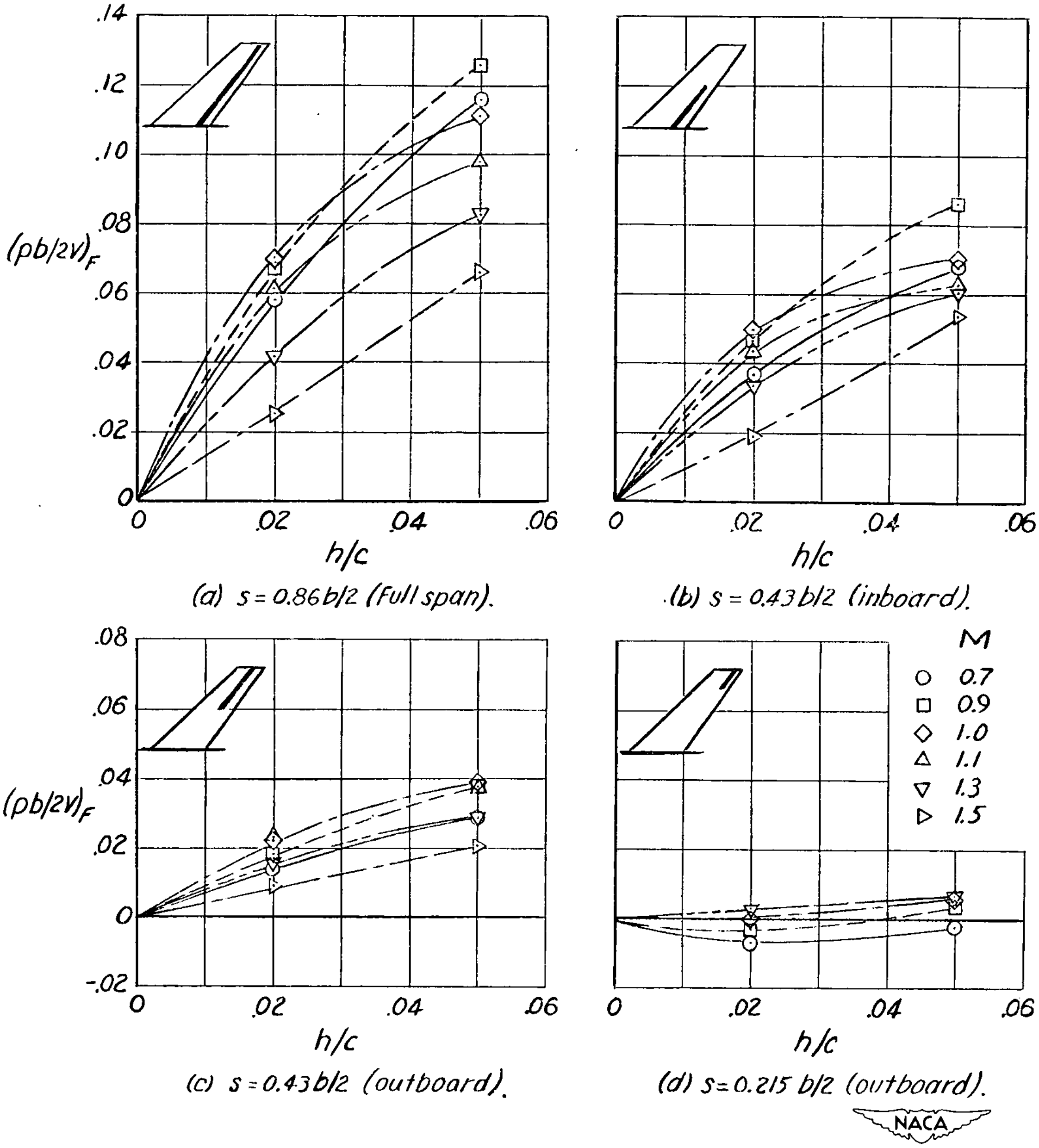

Figure 9.- Variation of rolling effectiveness with spoiler projection at constant Mach number. Type A wing structure.

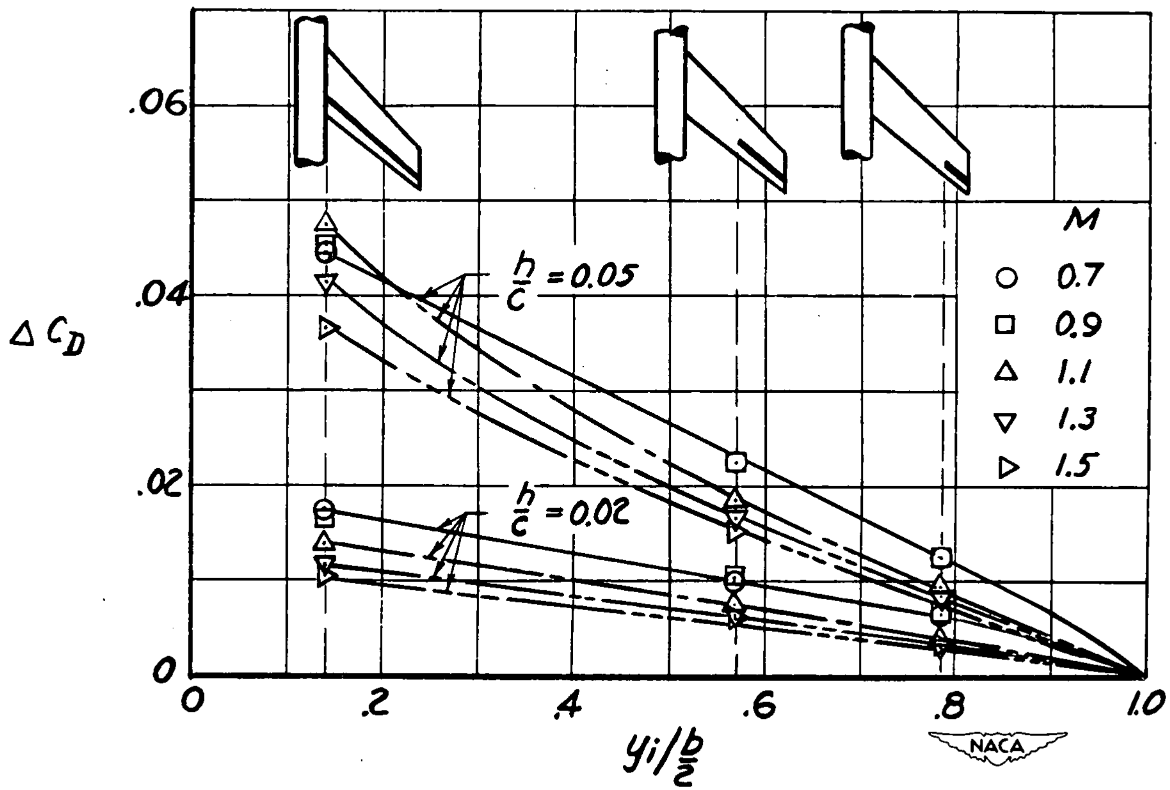

Figure 10.- Incremental spoiler drag coefficient plotted as a function of outboard spoiler span for both projections tested. Type A wing structure.

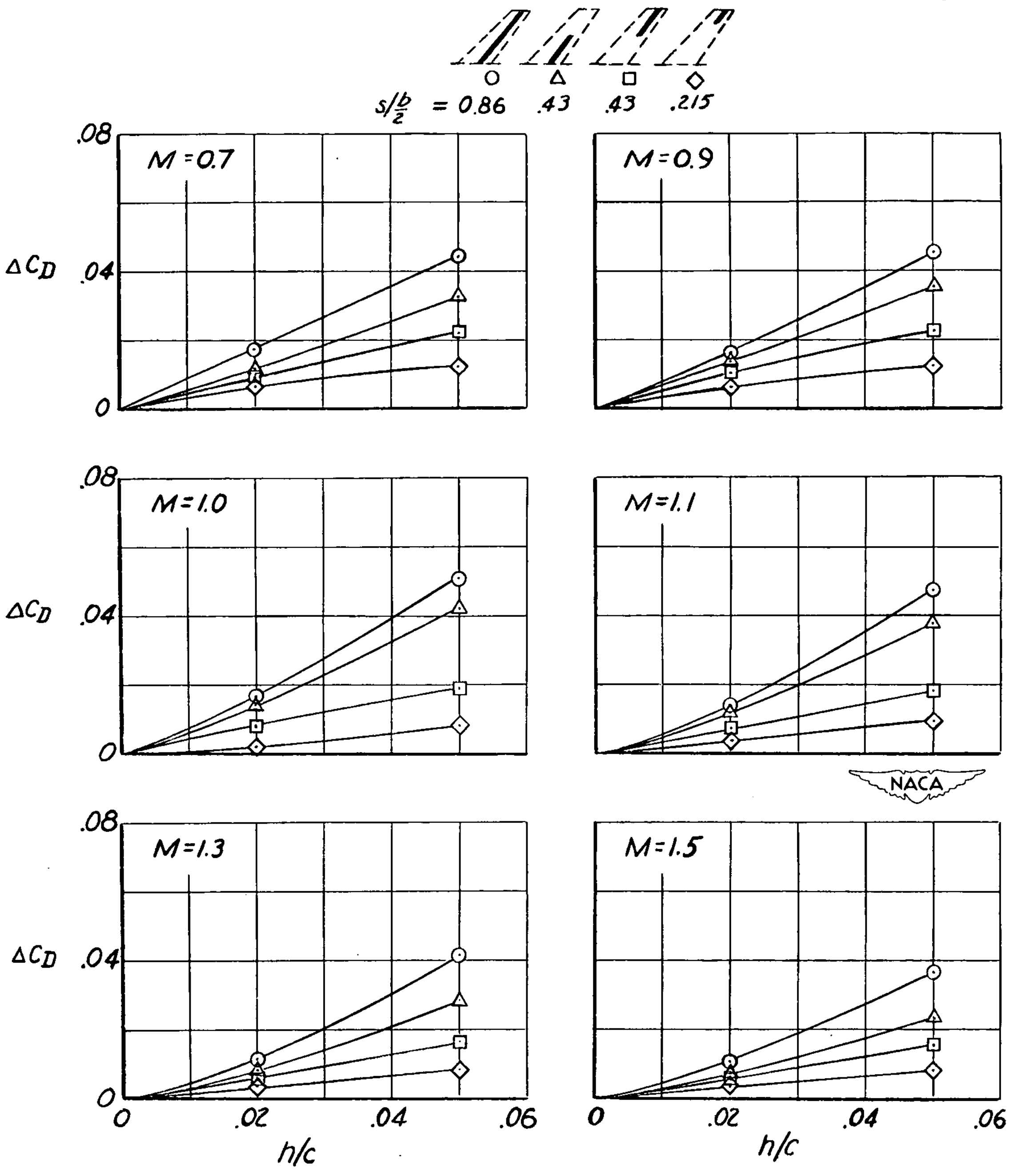

Figure 11.- Variation of incremental spoiler drag coefficient with spoiler projection at several test Mach numbers. Type A wing structure.

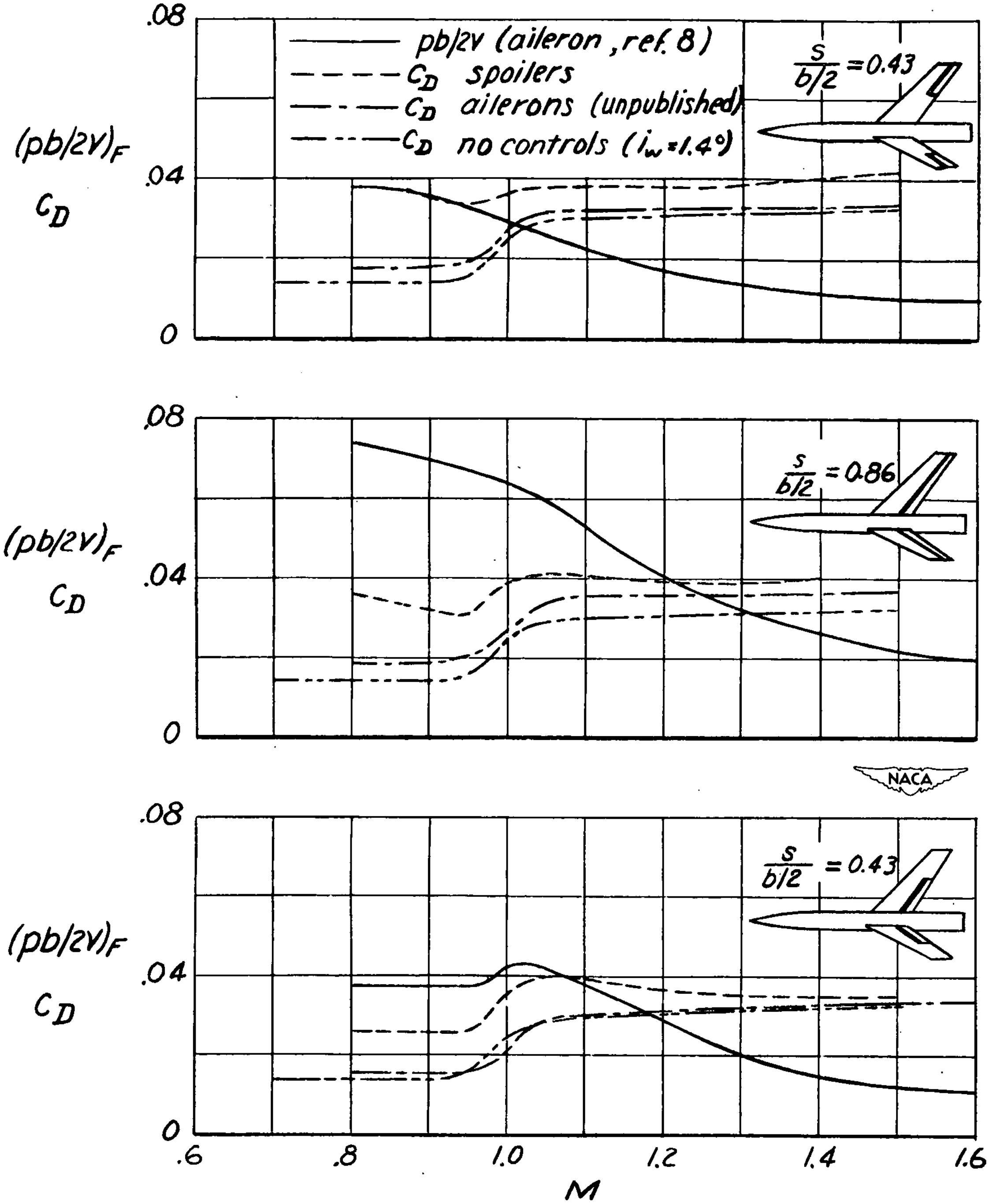

Figure 12.- Comparison of the total drag coefficients between model configurations having either spoiler or aileron-type controls at the same pb/2V over the Mach number range. $\frac{c_a}{c} = 0.30$; $\delta = 5^{\circ}$; h/c varies; wing structure A.

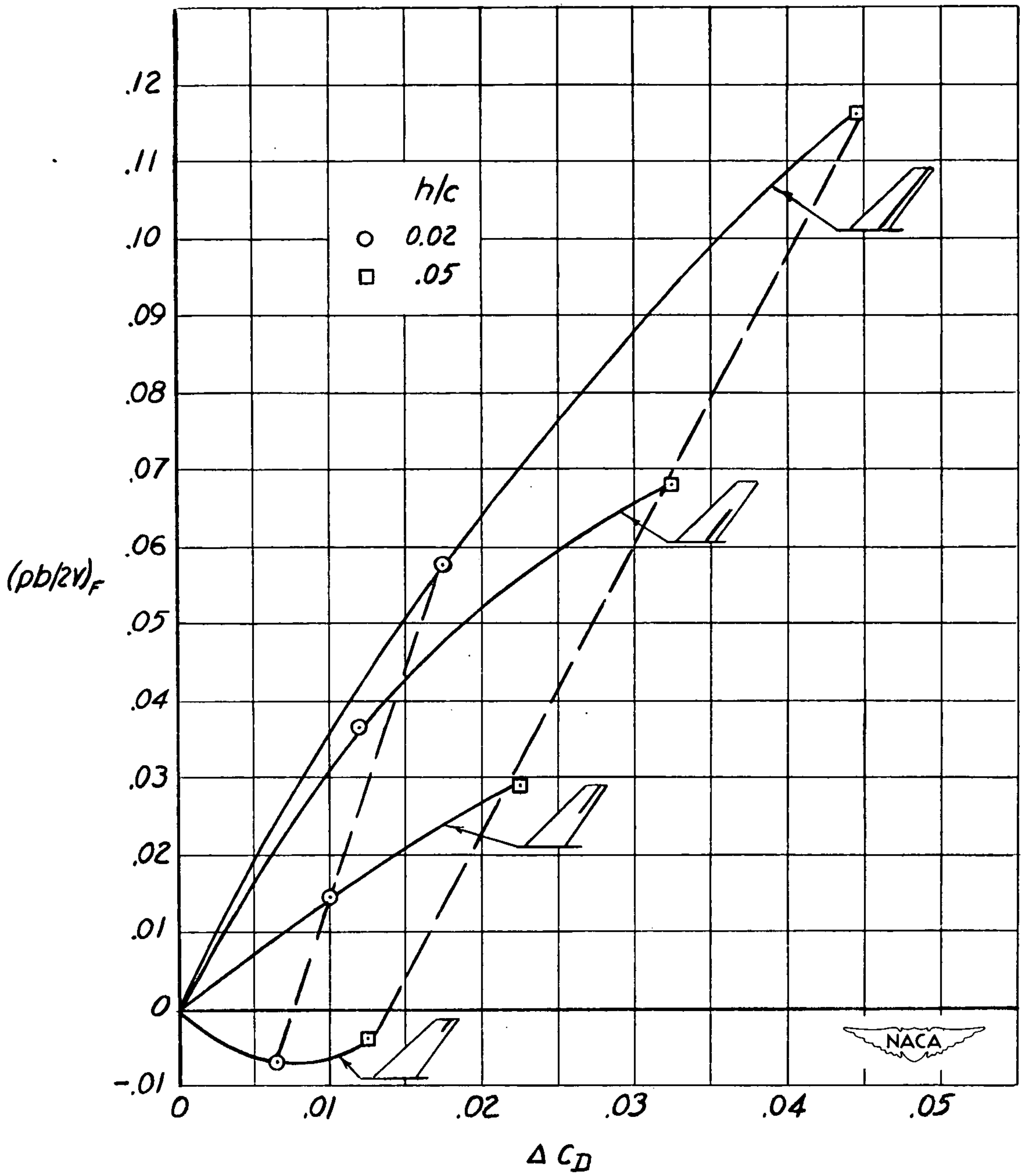

(a) M = 0.7.

Figure 13.- Variation of rolling effectiveness with incremental spoiler drag coefficient at constant Mach number. Type A wing structure.

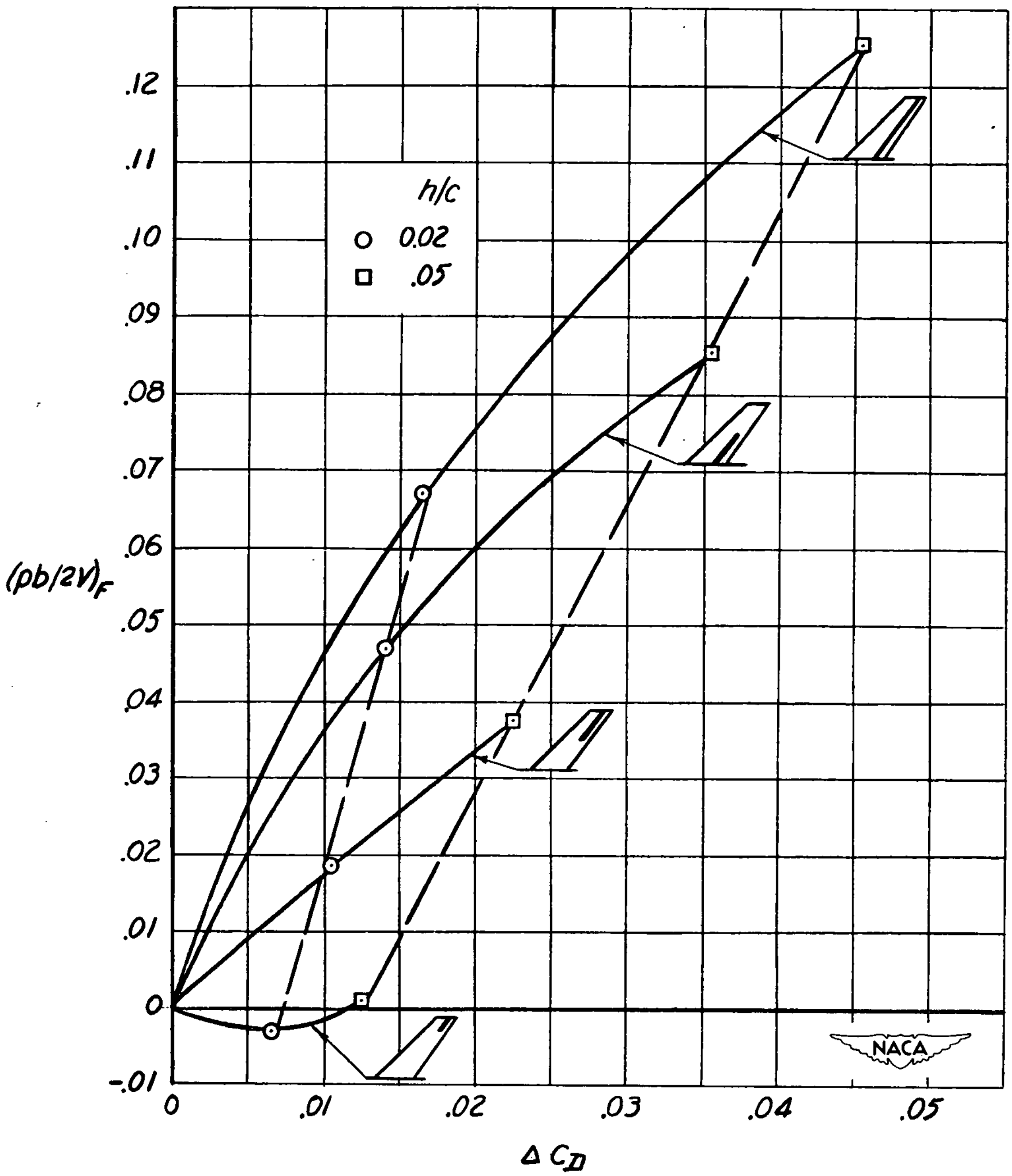

(b) M = 0.9.

Figure 13.- Continued.

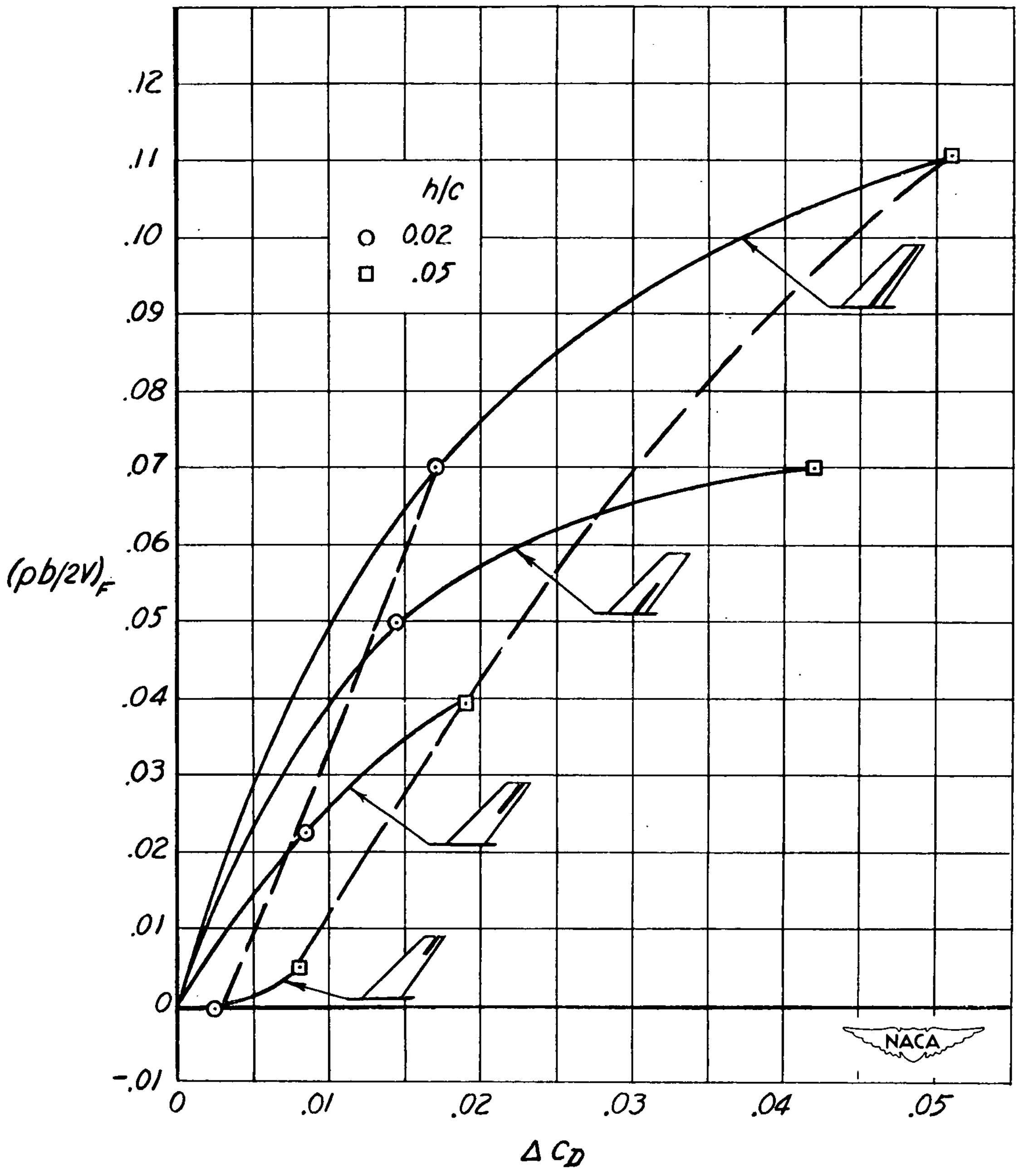

(c) M = 1.0.

Figure 13.- Continued.

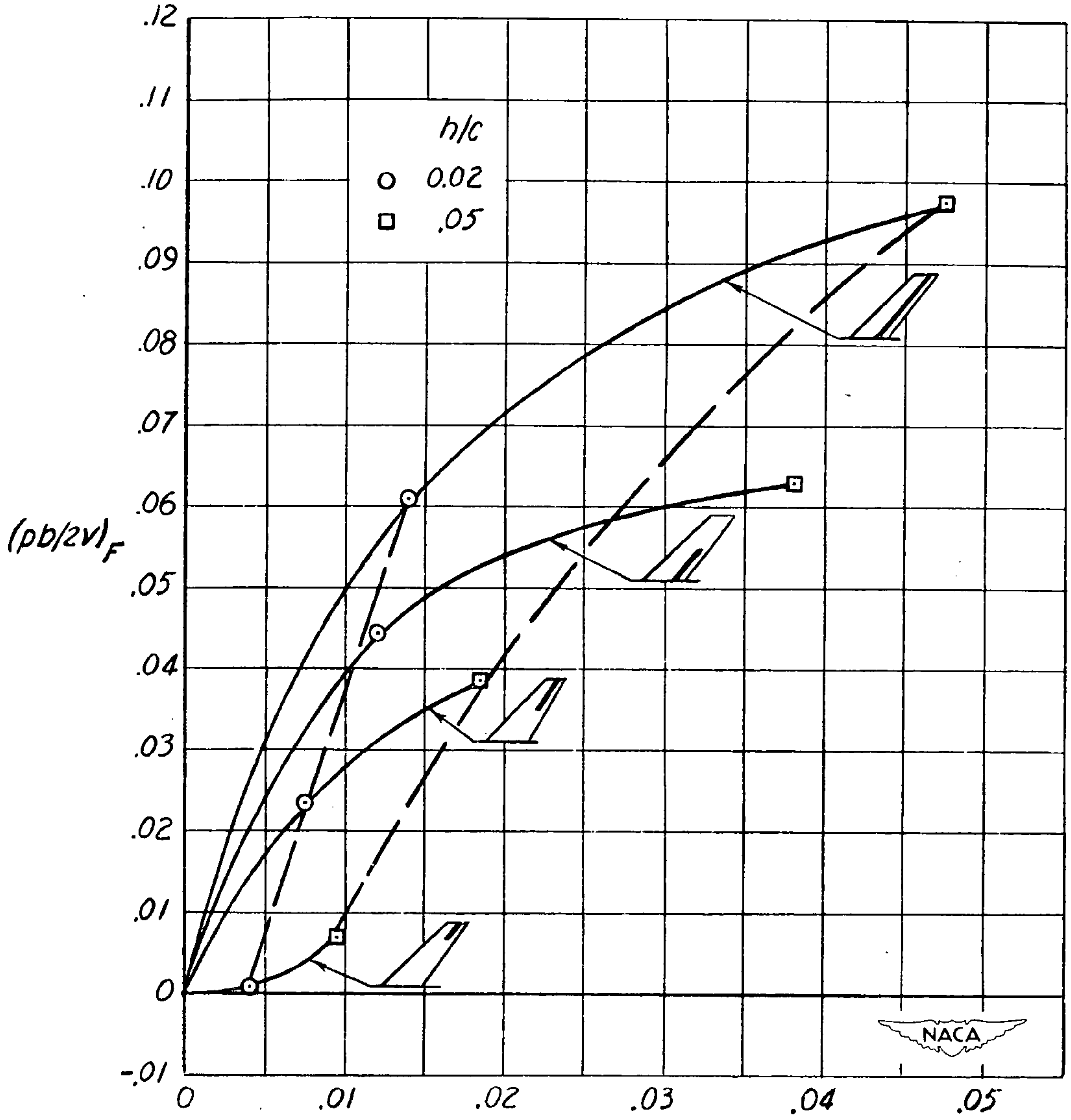

(d) M = 1.1.

Figure 13.- Continued.

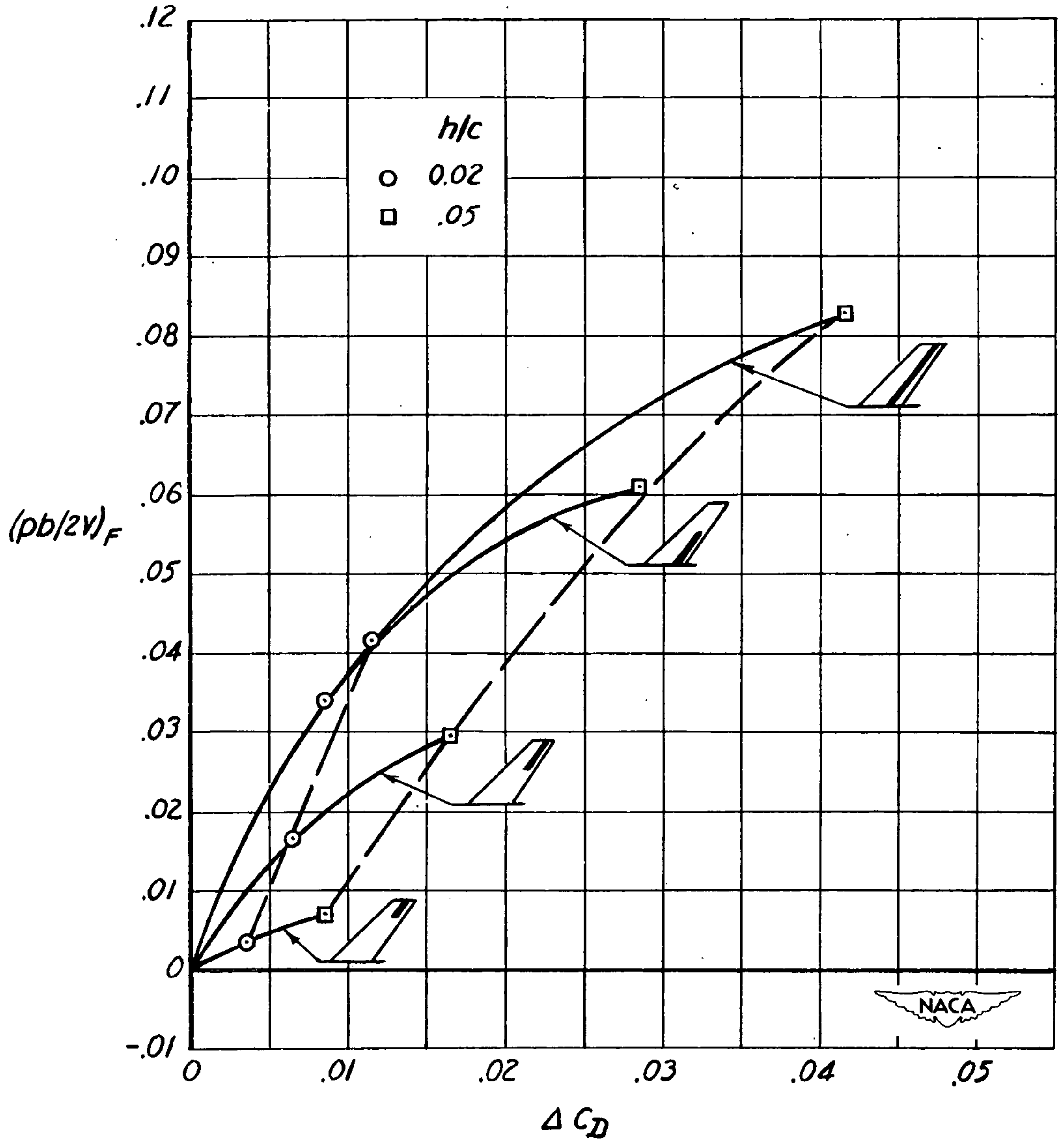

(e) M = 1.3.

Figure 13.- Continued.

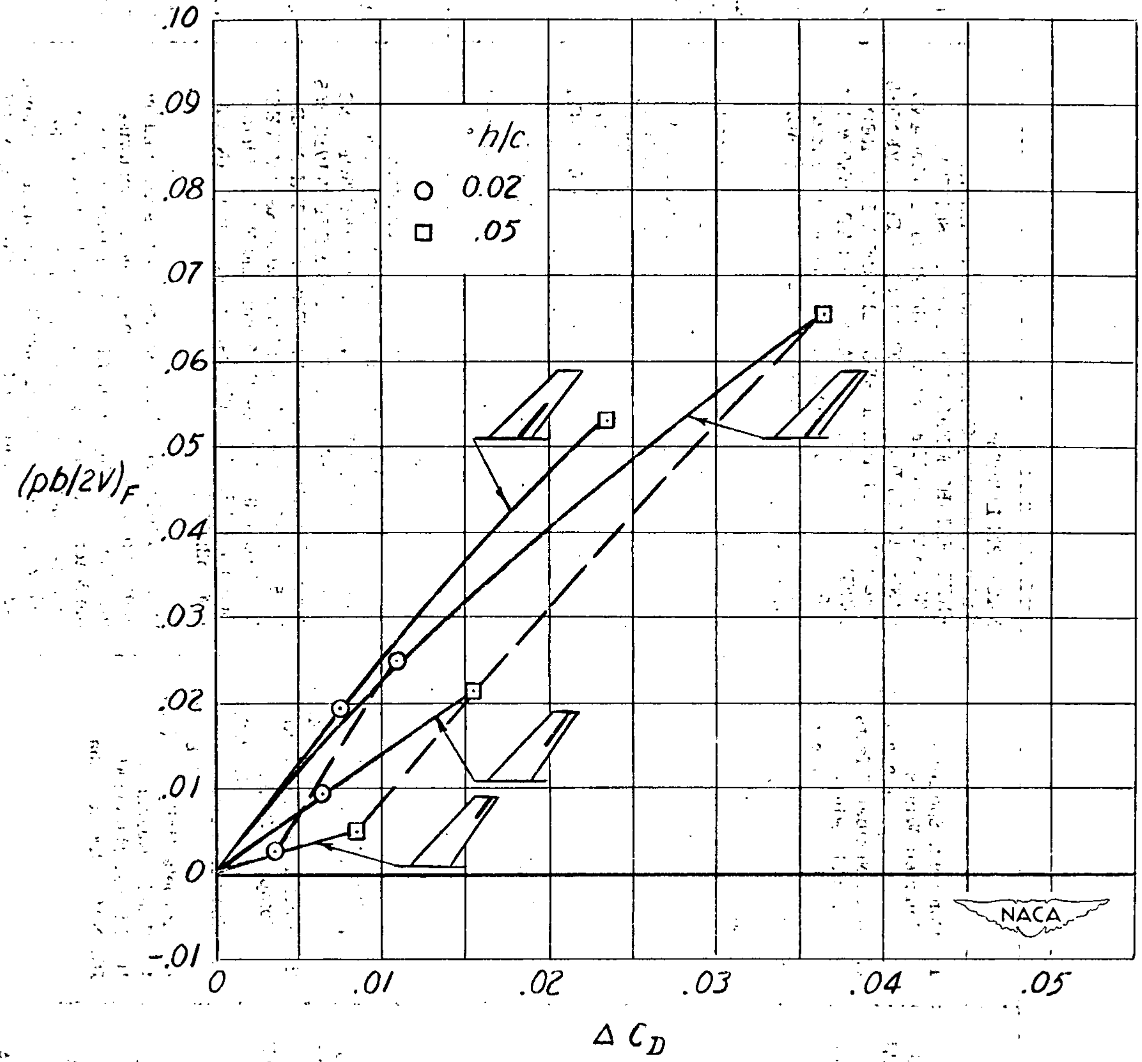

(f) M = 1.5.

Figure 13.- Concluded.